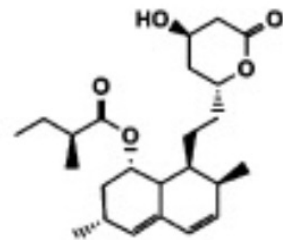


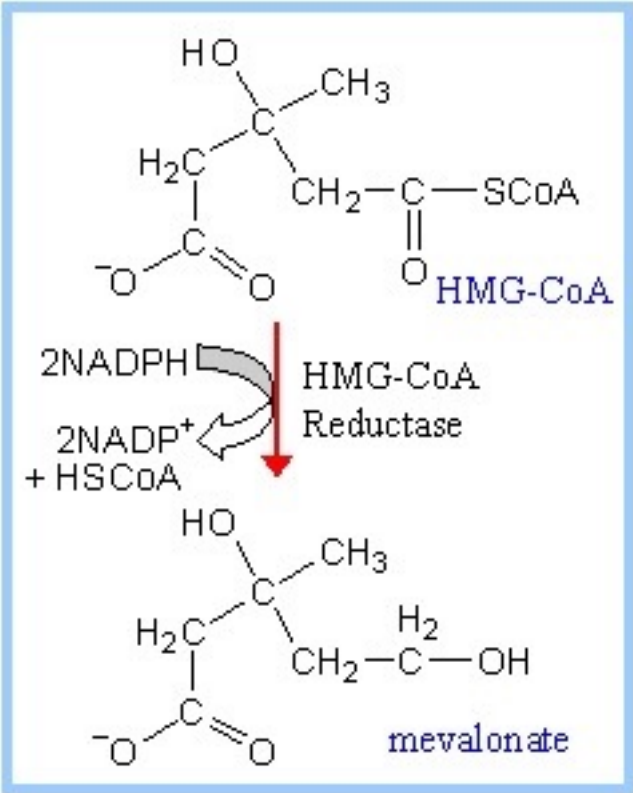
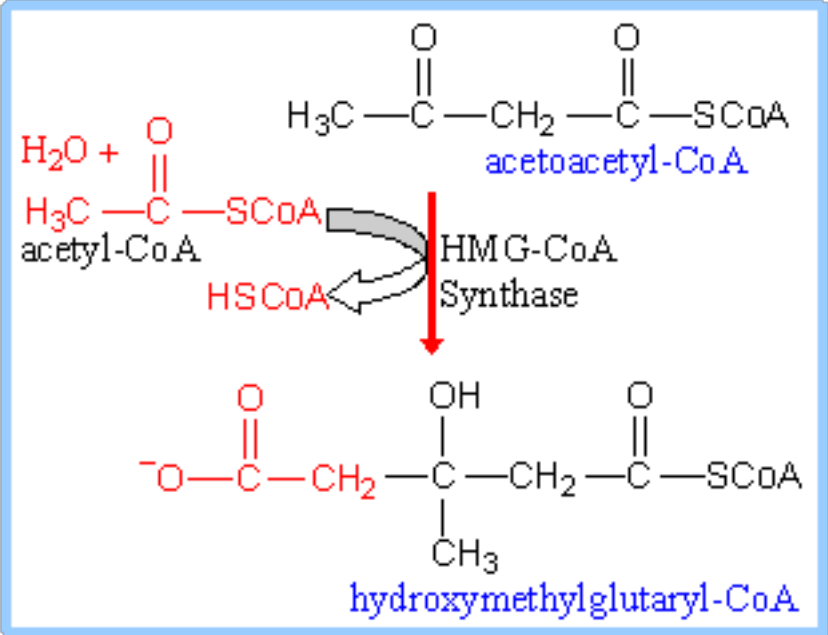
Structural basis of lovastatin biosynthesis

LovB PKS and the LovB-LovC complex



lovastatin
Aspergillus terreus
anticholesterol polyketide

Synthesis of mevalonate, the precursor of cholesterol



Role of statins: HMG-CoA reductase inhibitors

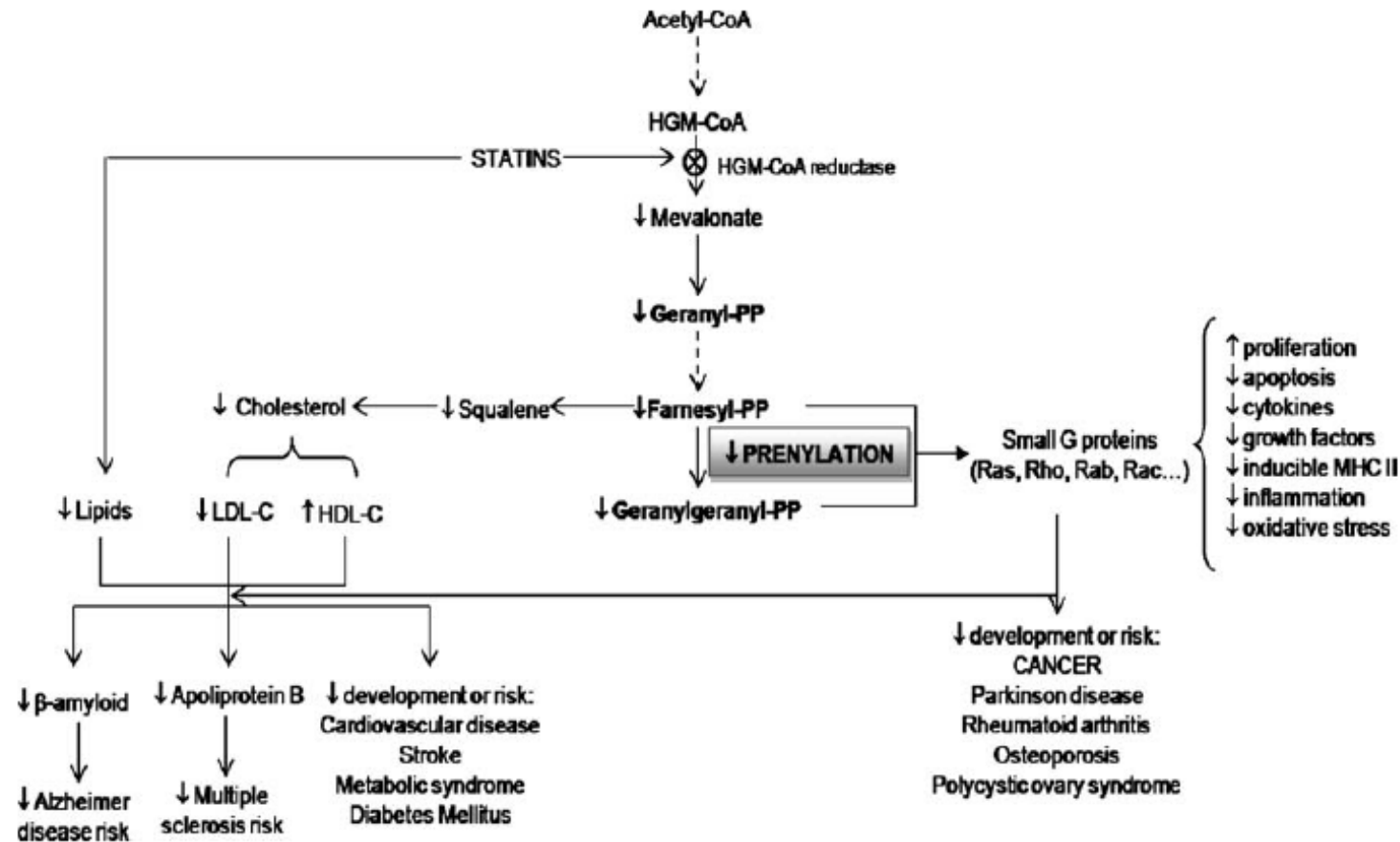


Fig. 5 Model explaining the great variety of biological effects of statins; and hence, current and potential uses. Inhibition of HMG-CoA reductase not only reduces cholesterol levels, but also of isoprenoid intermediates, affecting G proteins (i.e., Ras) prenylation. This can result in the modulation of signal transduction from receptors to gene

expression, directly affecting proliferation/apoptosis balance, inflammatory chemokines, and the cytogenic messages mediated by G proteins. Modified from: Cummings and Bauer 2000; Davignon and Leiter 2005; Massy and Guizarro 2001

Structure of HMG-CoA reductase with substrates or statins

Statins are competitive inhibitors of substrate HMG-CoA, not of NADPH

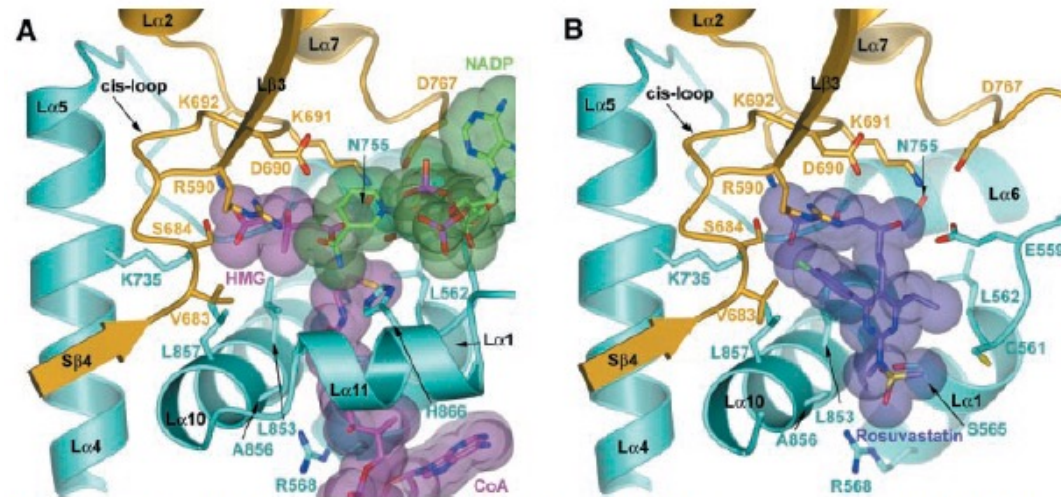
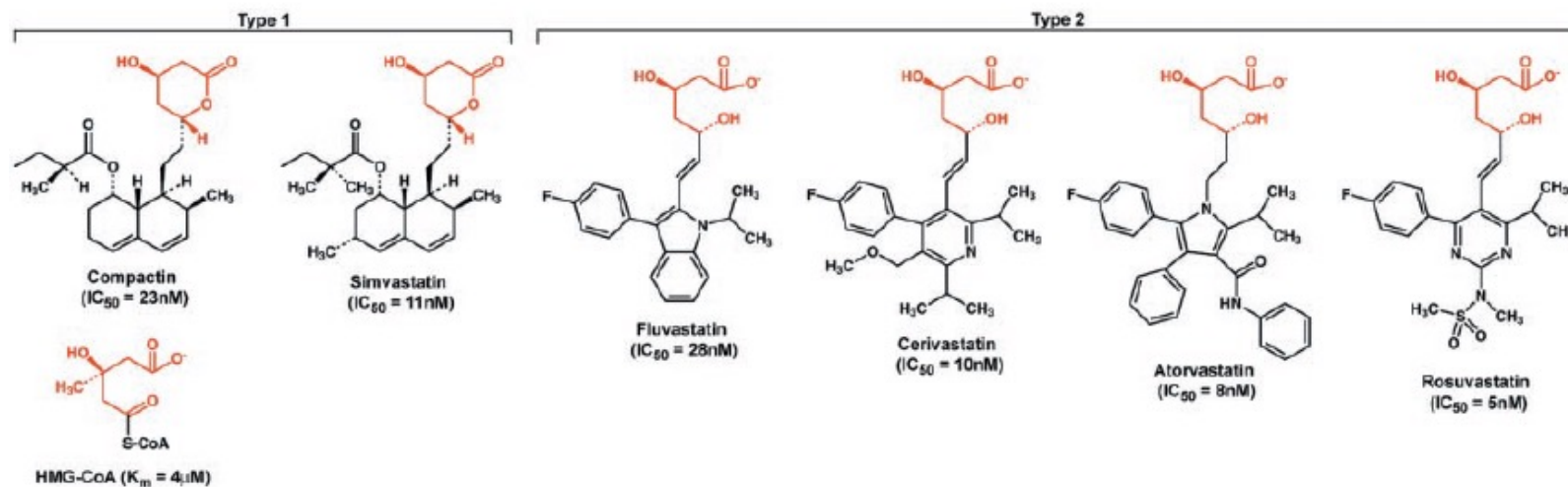
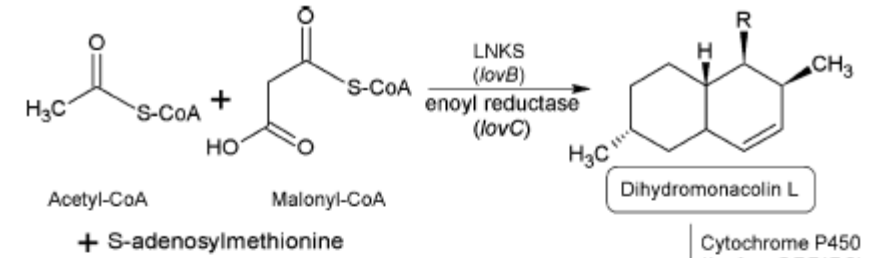
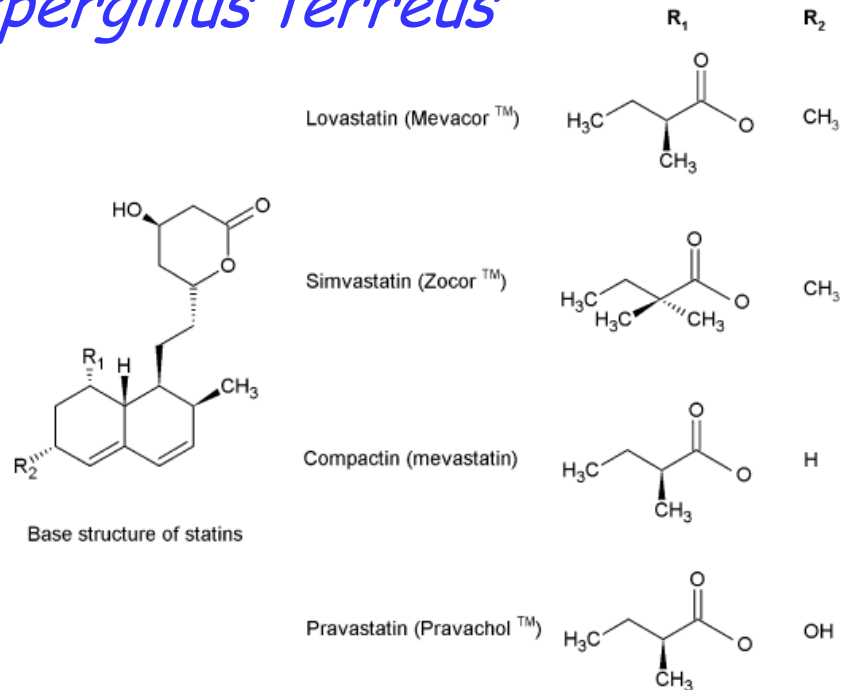


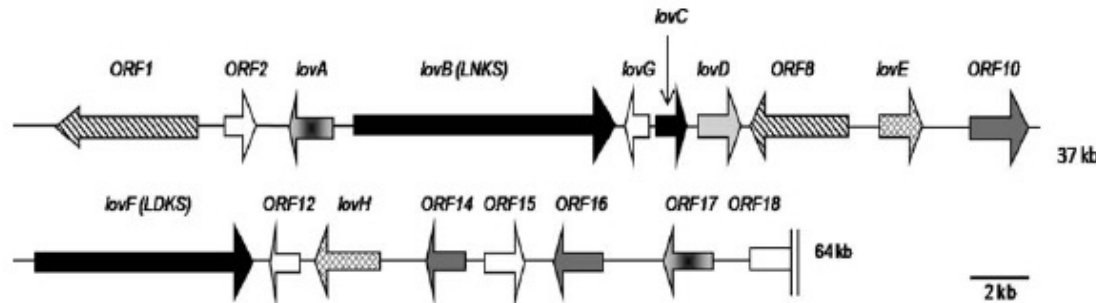
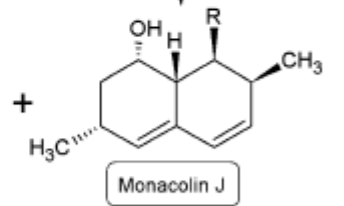
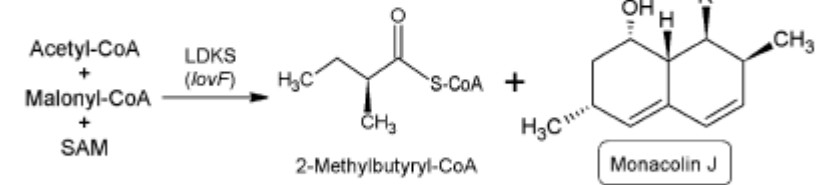
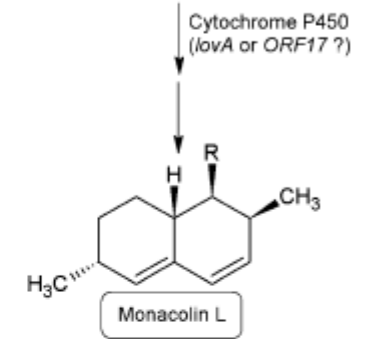
Fig. 2. Statins exploit the conformational flexibility of HMGR to create a hydrophobic binding pocket near the active site. (A) Active site of human HMGR in complex with HMG, CoA, and NADP. The active site is located at a monomer-monomer interface. One monomer is colored yellow, the other monomer is in blue. Selected side chains of residues that contact the substrates or the statin are shown in a ball-and-stick representation (20). Secondary structure elements are marked by black labels. HMG and CoA are colored in magenta; NADP is colored in green. To illustrate the molecular volume occupied by the substrates, transparent spheres with a radius of 1.6 Å are laid over the ball-and-stick representation of the substrates or the statin. (B) Binding of rosuvastatin to HMGR. Rosuvastatin is colored in purple; other colors and labels are as in (A). This figure and Figs. 3 and 4 were prepared with Bobscript (22), GLR (23), and POV-Ray (24).



Biosynthesis of statins: lovastatin is produced by *Aspergillus terreus*



LovB is an **iterative** and **permutative** PKS with KS-MAT-DH-CMeT-KR-ACP-CON domains
LovC is an enoyl-reductase



⊗ Potential resistance genes, ● Polyketide biosynthesis, ○ Transesterase, ● Transporter genes,
⊗ Regulatory genes, ● Cytochrome P450 genes and ○ unknown function

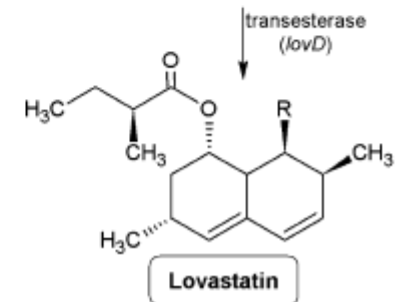


Fig. 3 Lovastatin biosynthetic gene cluster (modified from: Kennedy et al. 1999; Hutchinson et al. 2000)

Biosynthesis of lovastatin

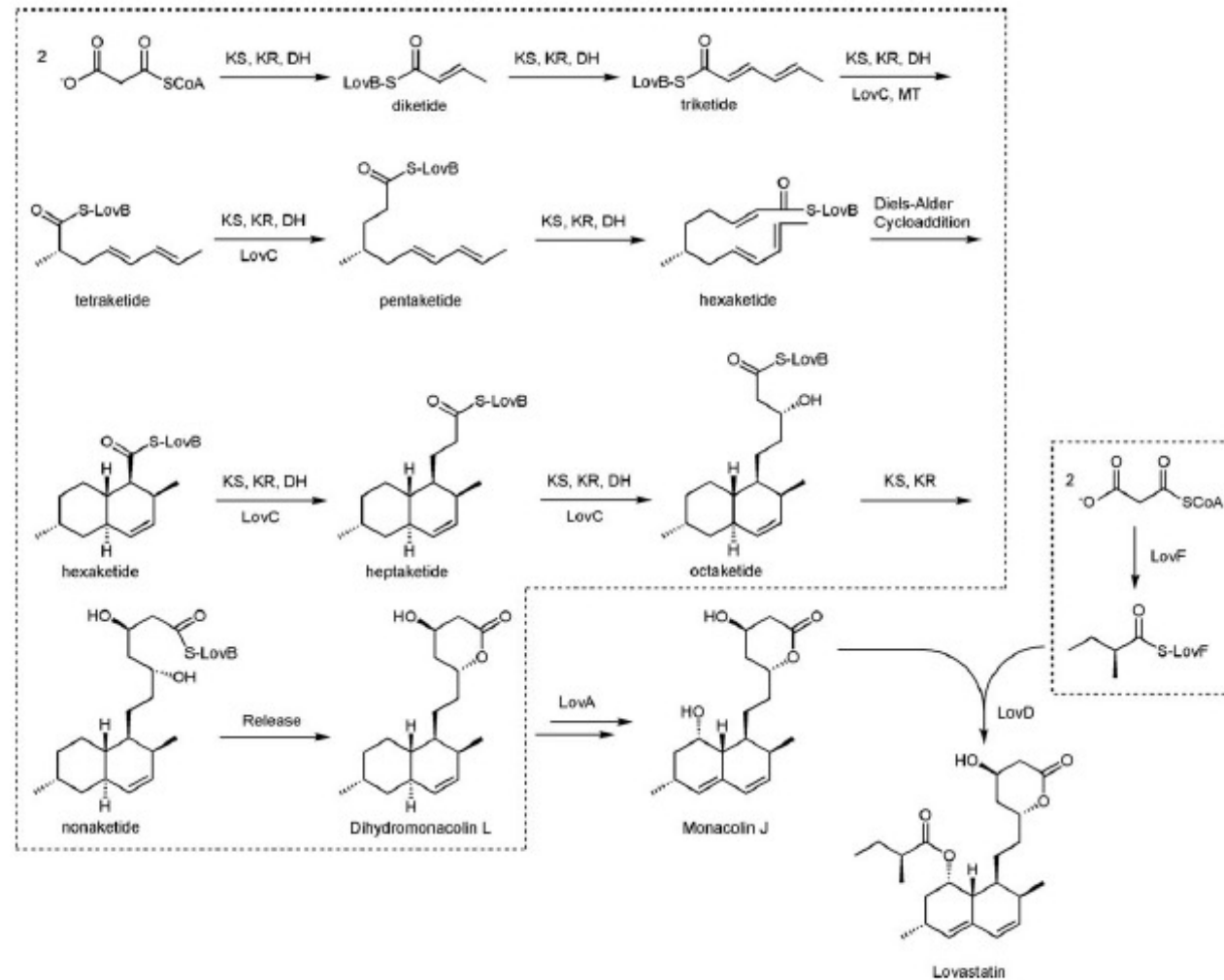
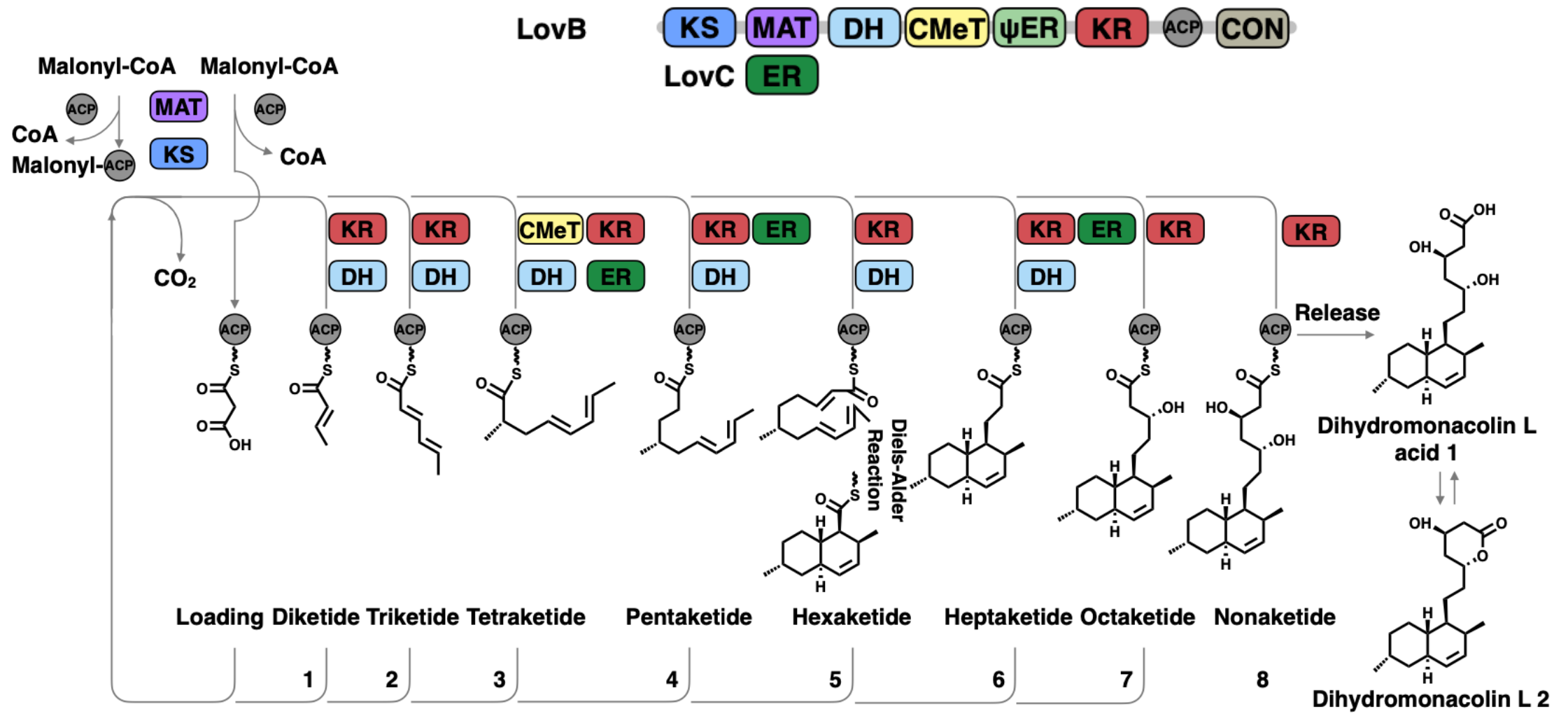


FIGURE 4 The proposed biosynthesis of lovastatin. The PKS steps are outlined by the dotted areas.

Biosynthesis of lovastatin

Role of LovB and LovC: synthesis of the nonaketide dihydromonacolin L







ARTICLE



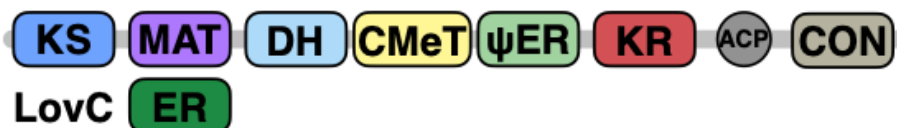
<https://doi.org/10.1038/s41467-021-21174-8>

OPEN

Structural basis for the biosynthesis of lovastatin

Jialiang Wang ^{1,4}, Jingdan Liang^{1,4}, Lu Chen¹, Wei Zhang¹, Liangliang Kong², Chao Peng ², Chen Su²,
Yi Tang³, Zixin Deng ^{1✉} & Zhijun Wang ^{1✉}

LovB

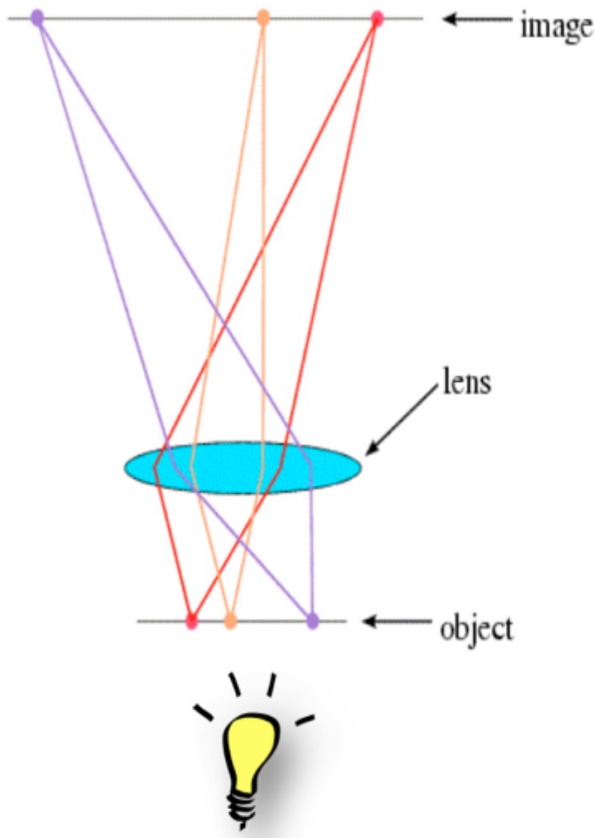


Statins are effective cholesterol-lowering drugs. Lovastatin, one of the precursors of statins, is formed from dihydromonacolin L (DML), which is synthesized by lovastatin nonaketide synthase (LovB), with the assistance of a separate *trans*-acting enoyl reductase (LovC). A full DML synthesis comprises 8 polyketide synthetic cycles with about 35 steps. The assembling of the LovB–LovC complex, and the structural basis for the iterative and yet permutative functions of the megasynthase have remained a mystery. Here, we present the cryo-EM structures of the LovB–LovC complex at 3.60 Å and the core LovB at 2.91 Å resolution. The domain organization of LovB is an X-shaped face-to-face dimer containing eight connected domains. The binding of LovC laterally to the malonyl-acetyl transferase domain allows the completion of a L-shaped catalytic chamber consisting of six active domains. This architecture and the structural details of the megasynthase provide the basis for the processing of the intermediates by the individual catalytic domains. The detailed architectural model provides structural insights that may enable the re-engineering of the megasynthase for the generation of new statins.

Methodology

- Recombinant expression of LovB (His-tag) in a *S. cerevisiae* strain expressing *A. terreus* *npgA* (4-PP transferase)
 - 6 mg protein from 50 gr cells
- Recombinant expression of LovC (His-tag) in *E. coli* BL21(DE3)
 - 3 mg protein from 5 gr cells
- Purification with Ni-NTA resin
- Enzyme activity assays
 - Synthesis of DML, NADPH consumption
- Determination of the structure of LovB and of the LovB-LovC complex by **cryoEM**
- Identification and analysis of the LovB_MAT-LovC interaction interface

From optical microscopy to cryoEM



Refraction (or Dispersion)

Change of propagation rate in a different medium causes a change in the incident angle (Snell law)

Resolution increases as radiation wavelength employed decreases

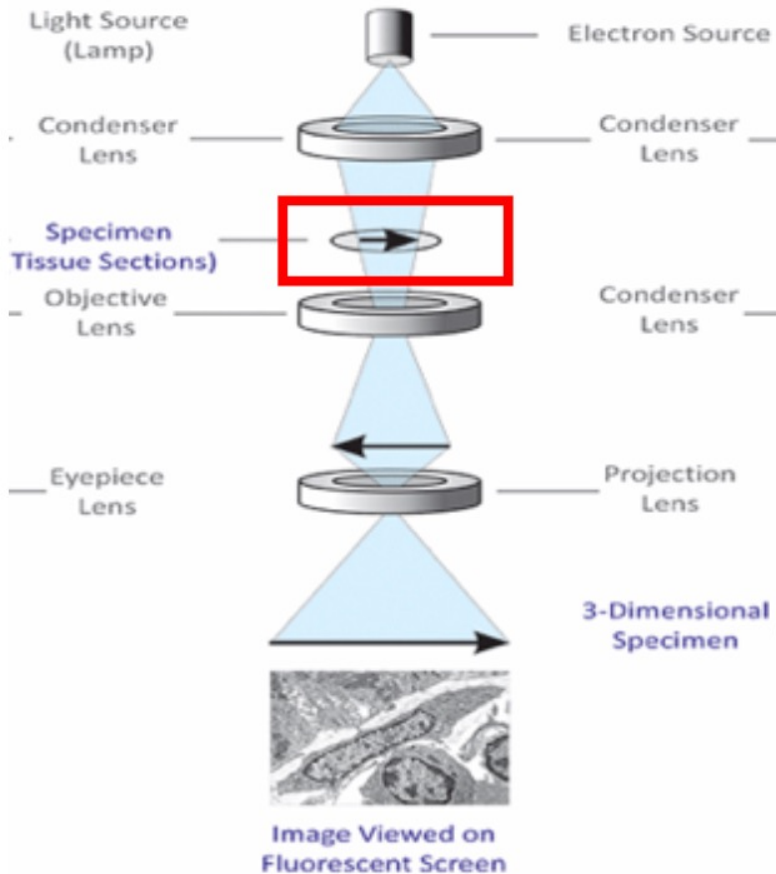
The resolution limit of the optical microscope is linked to the wavelength of the radiation employed

[λ PHOTONS = 400-600 nm]

$$\Delta x \cong \frac{\lambda}{2n \sin \alpha}$$

The discovery that electrons are endowed with very-low wavelength radiation [λ ELECTRONS = tens of picometers] suggested the possibility to use electron beams to obtain much higher resolution

CryoEM methodology



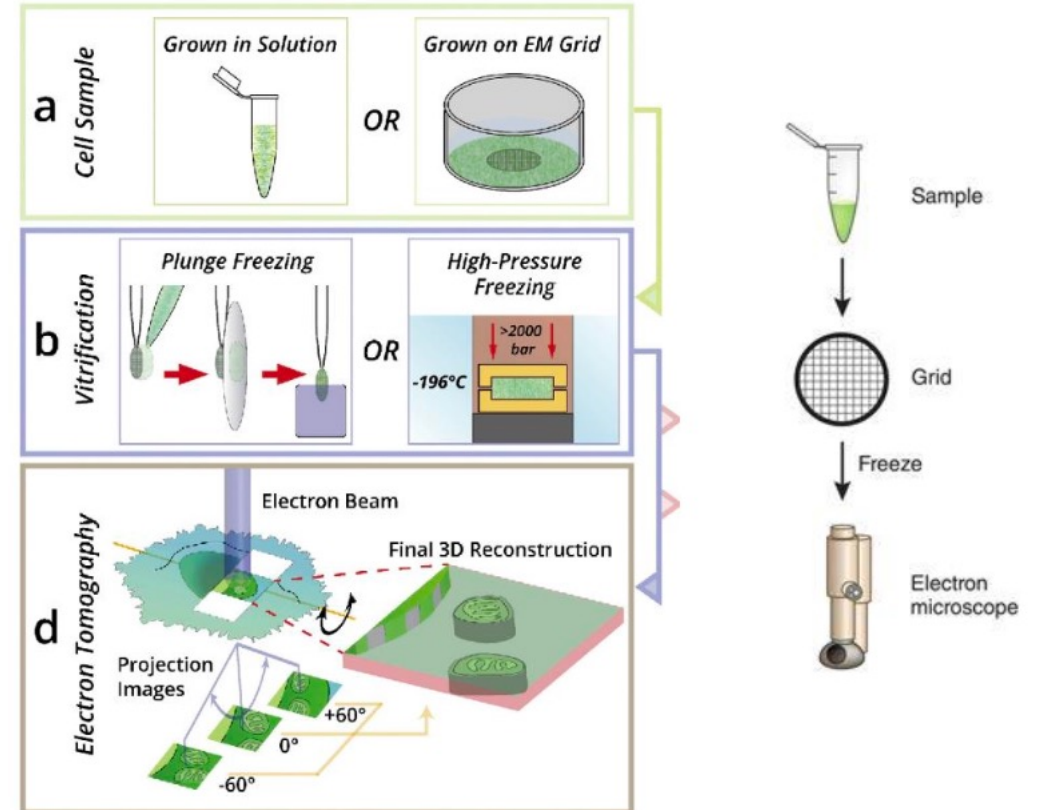
CryoEM: resolution limit 1-10 nm

Optical microscopy: resolution limit 1 μm

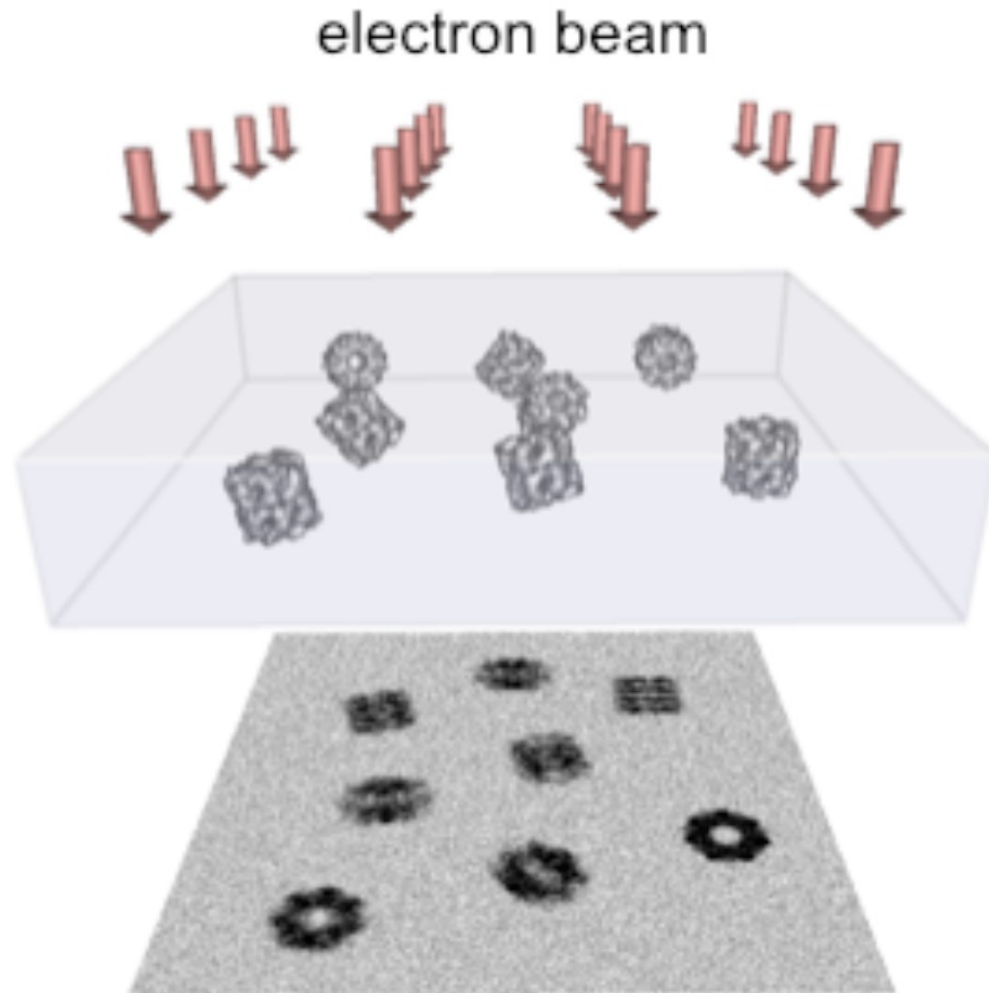


CryoEM methodology

- Penetration power of the electron beam is limited → **thin sections** (50-500 nm)
- The lower the wavelength of electromagnetic radiation, the higher the energy that is transferred to the sample → **radiation damage**
- Water in living matter is highly conducive → **dried sample**
- The biological sample is deposited on a metal grid and it is rapidly frozen
- Analysis is performed at cryogenic temperature (77 K, -196° C)



CryoEM methodology



The biological sample is analyzed at **cryogenic temperature** (77 K \rightarrow -196° C)

ADVANTAGES

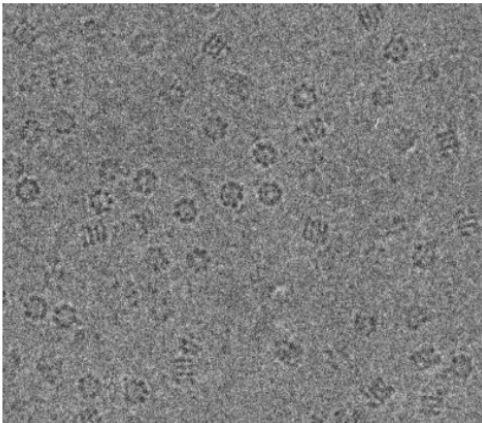
- Reduction of background of the biologic matrix (reduced molecular vibrations because of low temperature)
- Stabilization of the sample
- Stability of macromolecular structures
- Heterogeneity of orientation of the sample with respect to the electron beam
- Reduction of amount of sample

ACHIEVABLE RESULTS

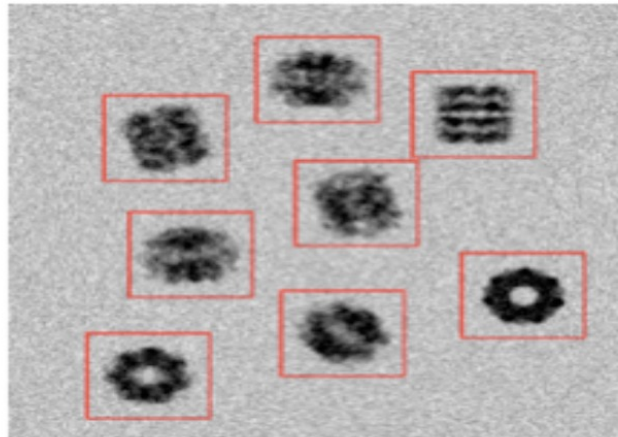
- Electron tomography of cellular organelles at resolution $<40 \text{ \AA}$
- Analysis of SINGLE macromolecular complexes at resolution $<5 \text{ \AA}$
- Determination of the structure of membrane proteins

CryoEM methodology: single particle analysis

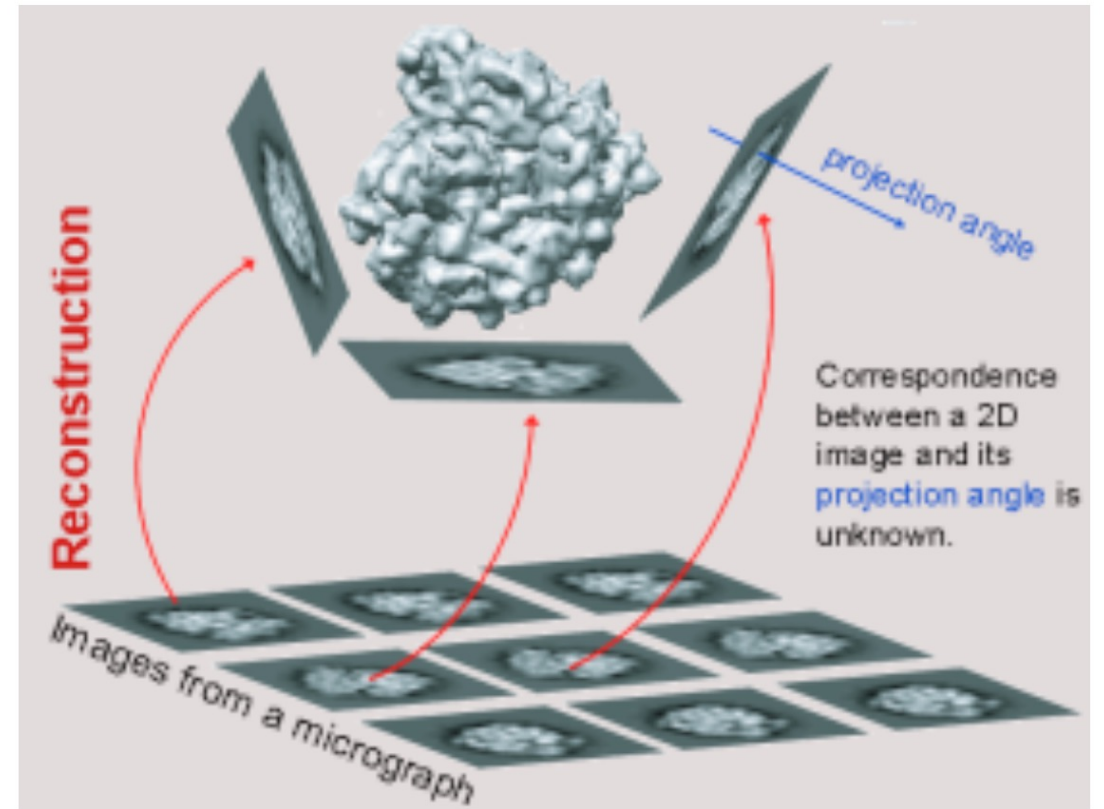
1. collect micrographs



2. digitally select particle images

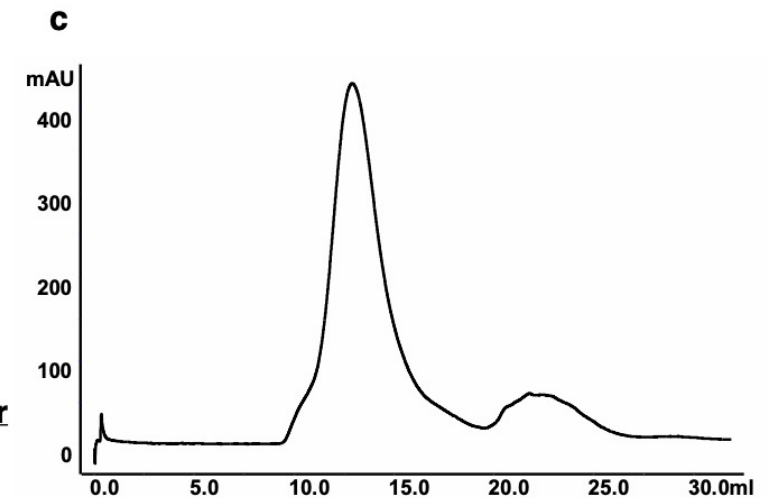
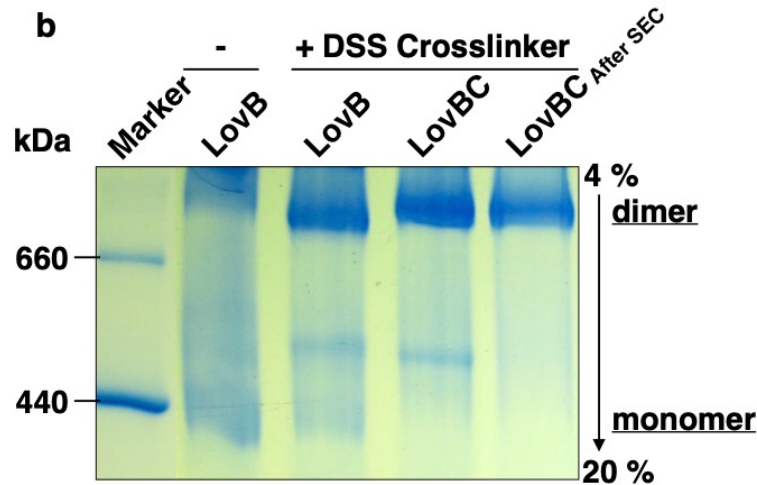
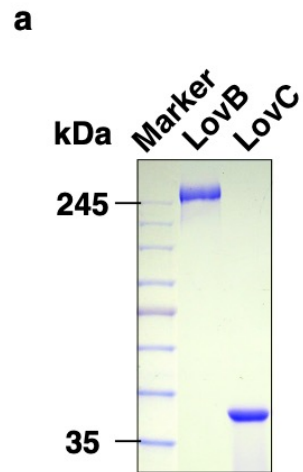
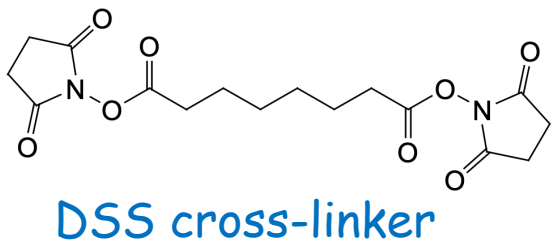


3. reconstruct 3D structure from 2D images



Methodology

- Preparation of the LovB-LovC complex: stabilization with DSS and purification by gel-filtration chromatography on Superose 6 (molecular weight of LovB 250 kDa, LovC 40 kDa)



CryoEM micrographs of the LovB-LovC complex

Cofactors!!!

NADPH

SAM

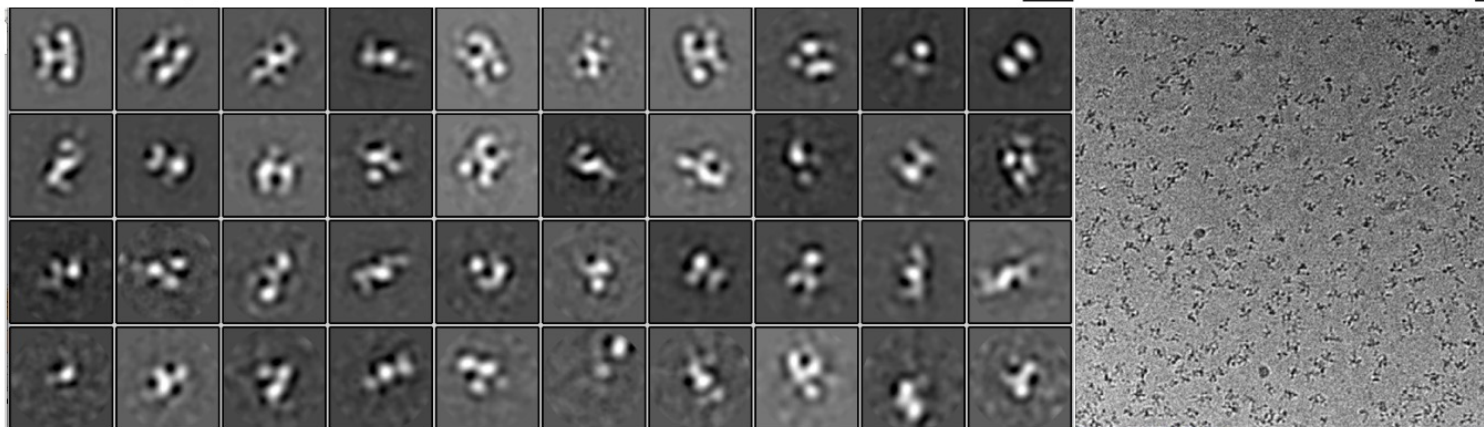
Malonyl-CoA

Immediately prior to specimen preparation, Tween 20 (10%) was added to the freshly purified LovBC complex to a final concentration of 0.1%, which improved the quality of vitreous ice in the specimen. Four microliter aliquots of specimen at ~8 mg/ml were applied to glow-discharged holey carbon grids (Quantifoil Cu, R1.2/1.3, 200 mesh) for 60 s of incubation and then blotted for 2.5 s and plunge-frozen into liquid ethane pre-cooled by liquid nitrogen using a Vitrobot Mark IV (FEI) operated at approximately 100% humidity and 22 °C. Cryo-EM images were collected with a Titan Krios electron microscope (FEI) operated at 300 kV and equipped with a K2 Summit direct electron detector (Gatan).

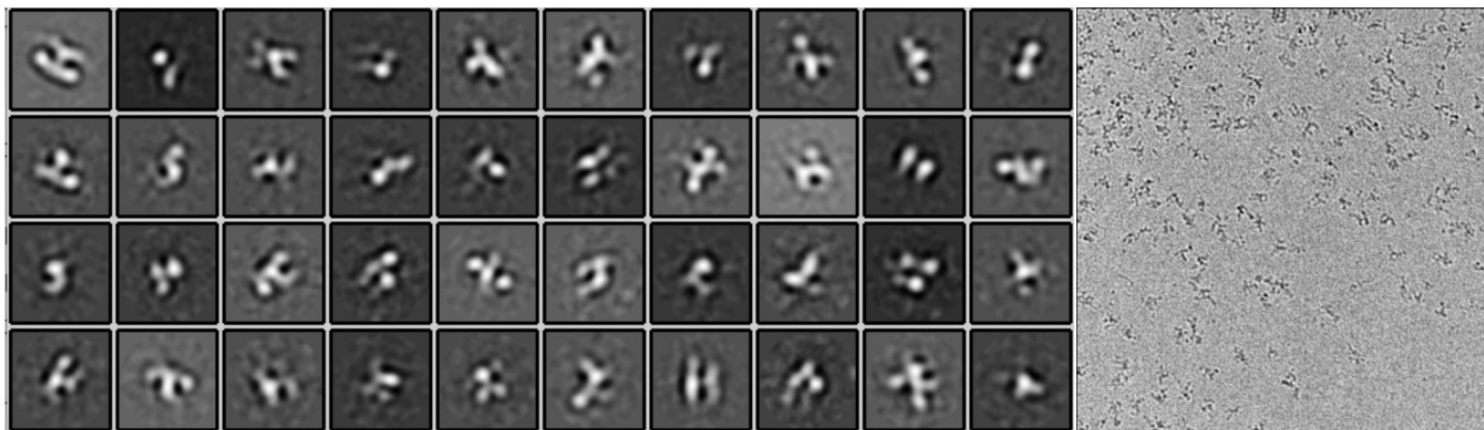
LovBC_added with cofactors

20 nm

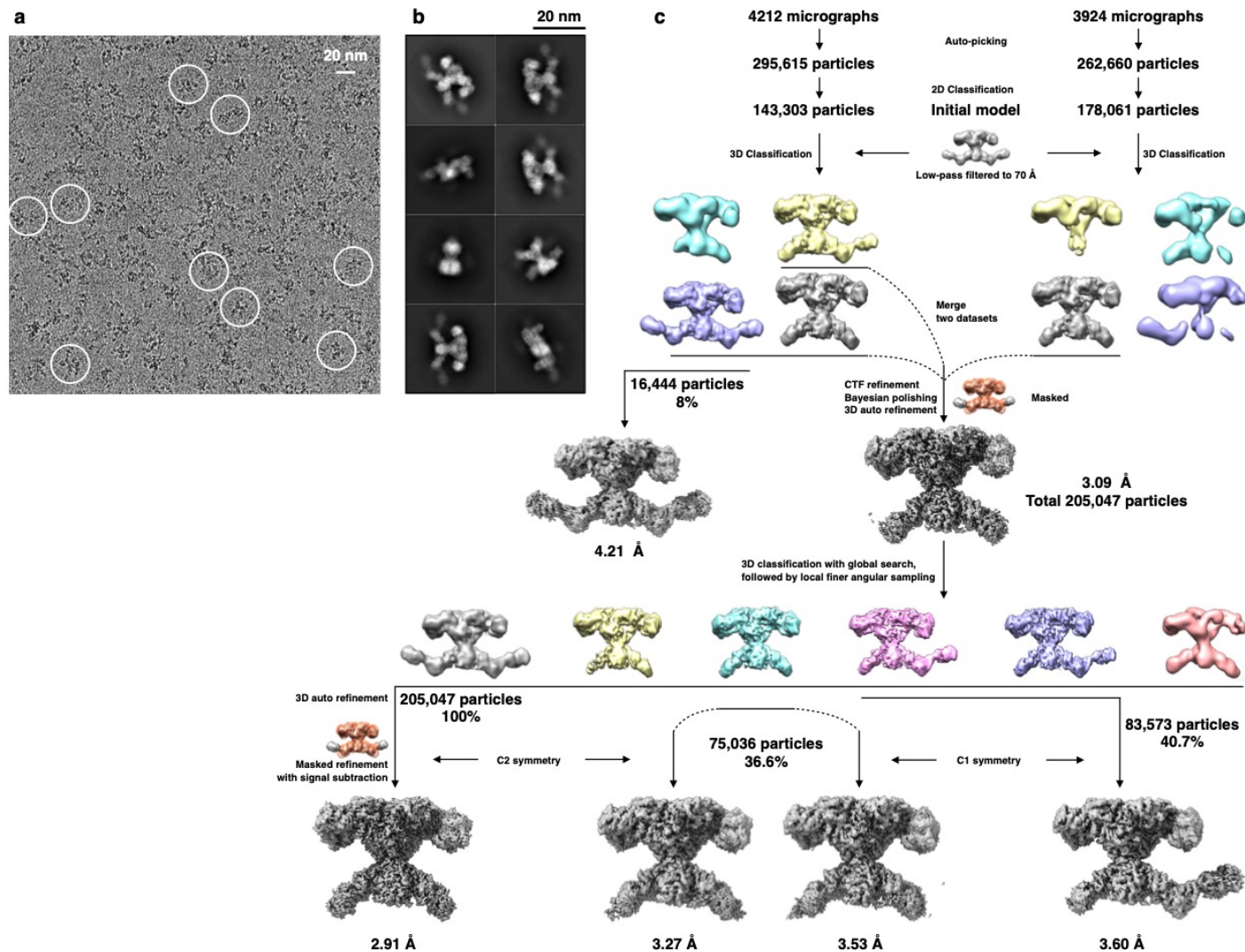
20 nm



LovBC_no cofactors



cryoEM data analysis



Supplementary Fig. 4 Cryo-EM structure determination of the LovBC complex. **a** One representative cryo-EM micrograph from the 8136 movie stacks of the LovBC complex with selected particles in white circles. Scale bar, 20 nm. **b** Eight representative 2D class averages of the LovBC complex from 100 averages. Scale bar, 20 nm. **c** A data processing workflow for the resolution-labeled density maps.

Molecular architecture of LovB and the LovB-LovC complex

- LovB is an X-shaped dimer
- LovC is associated to the MAT domain of LovB
- LovB ACP and CON domains are not resolved in the structure
- Two L-shaped catalytic chambers are formed by KS-MAT from one subunit and DH-CMeT-KR from the other subunit

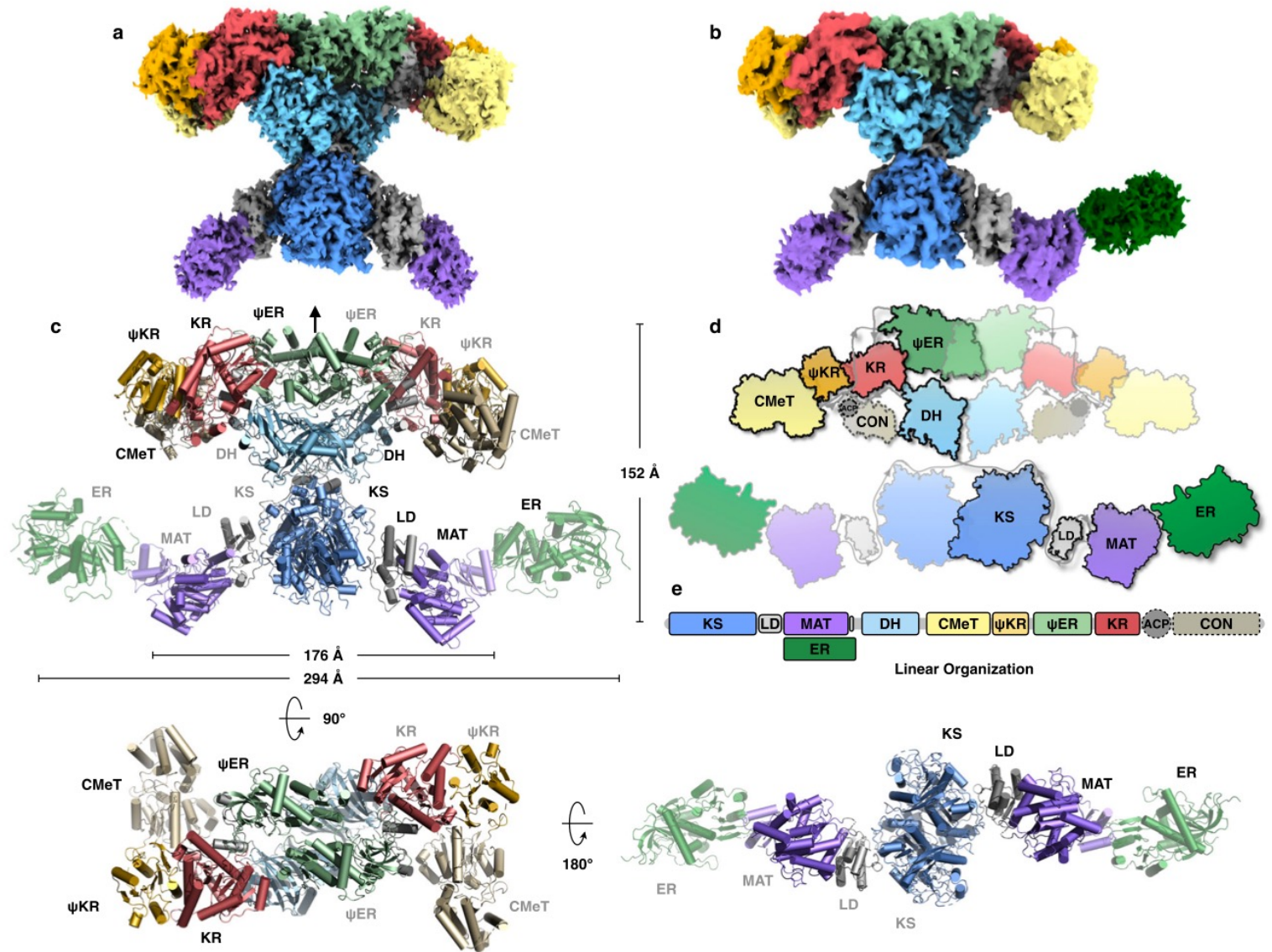


Fig. 1 Overall architecture of the LovBC complex. Cryo-EM density maps of LovB (a) at 2.91 Å and the LovBC complex (b) at 3.60 Å resolution with each domain colored uniquely. c The atomic model of the LovBC complex with the dimensions indicated is shown in front, top, and bottom views. The pseudo-twofold symmetry axis is indicated by an arrow. d Schematic diagram of the domain arrangements illustrating the X shape of LovBC. e Linear domain organization of the LovBC complex. The unresolved ACP and CON domains are bordered by dotted lines.

Structures of LovB domains: 'substrate tunnel' and active sites

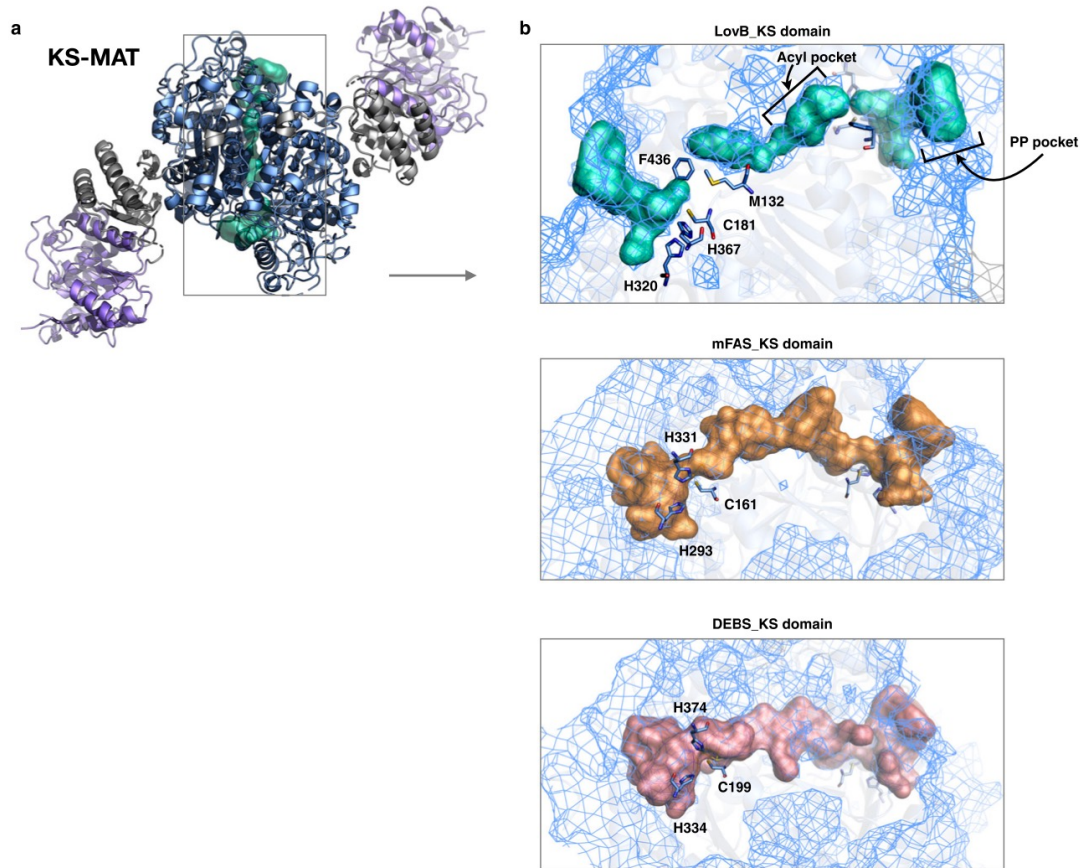


Fig. 2 The KS-LD-MAT domains of LovB. **a** The model of the domains is shown in top view, with the substrate binding tunnel represented in cyan surface. **b** Top, close-up view of the disconnected catalytic tunnel of KS. The conserved active site residues are labeled. Two additional residues (M132 and F436) intercept the acyl (inner) and PPant (outer) pockets. Middle and bottom, the long traversing-through substrate tunnels of KS domains from mFAS and DEBS.

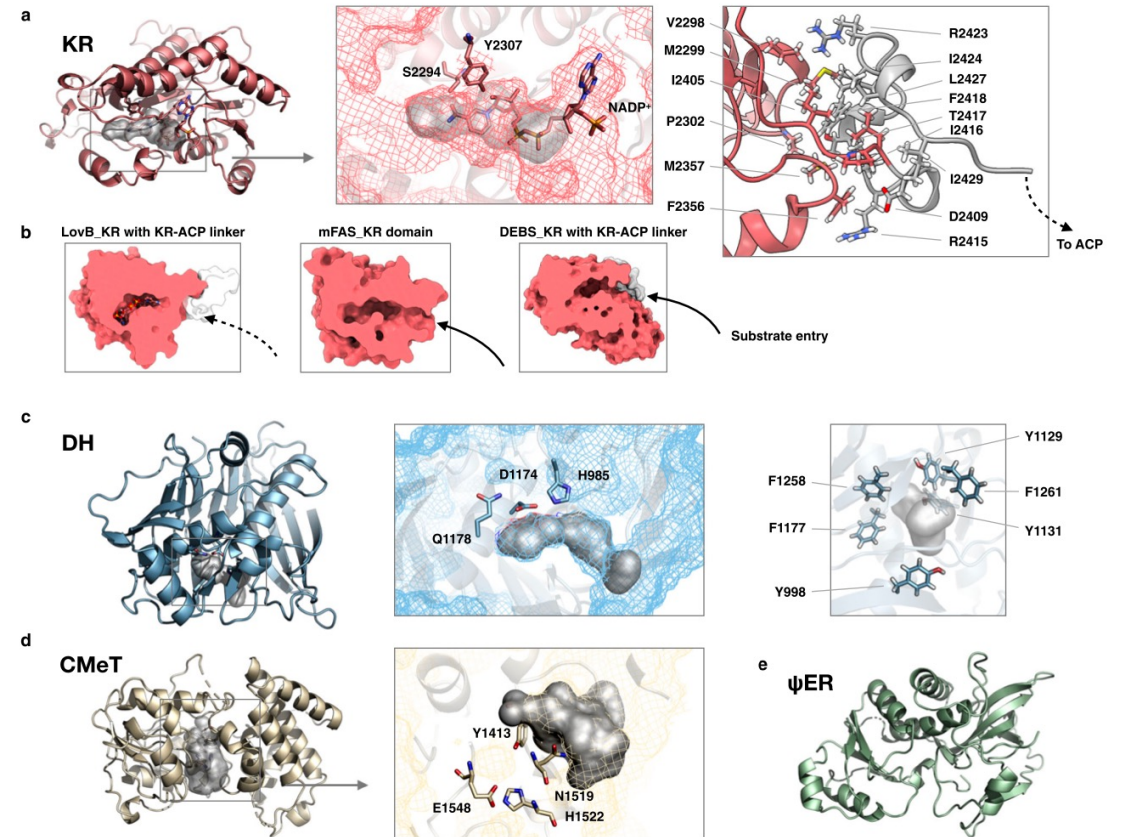


Fig. 3 Tailoring domains of LovB. **a** KR domain with bound cofactor NAD⁺, substrate tunnel (gray surface) and active site residues. Interacting residues of post-KR linker with KR are labeled. **b** Surface representation of KR with post-KR linker was cut perpendicularly to show the restricted substrate entry groove, compared with the groove for homologous KR domains from mFAS and DEBS. **c** Model of the DH domain. Active site residues are marked, and six aromatic amino acids along the substrate tunnel are highlighted on the right. **d** CMeT domain. Active site residues located between two subdomains are labeled, and the groove formed between the two subdomains is shown in gray surface. **e** ψER domain.

Interaction LovB_MAT-LovC

MAT-LovC interaction is essential for the synthesis of DML

- *In silico* and *experimental* analyses: identification of the interaction interface
- Mutant LovC (T271L, R272I, K273G, M274A) is active but unable to interact with MAT (gel-filtration chromatography)
- No DML formation is observed in the in vitro reaction LovB-LovC_{mut}

NOTE: the thioesterase LovG is added for product release

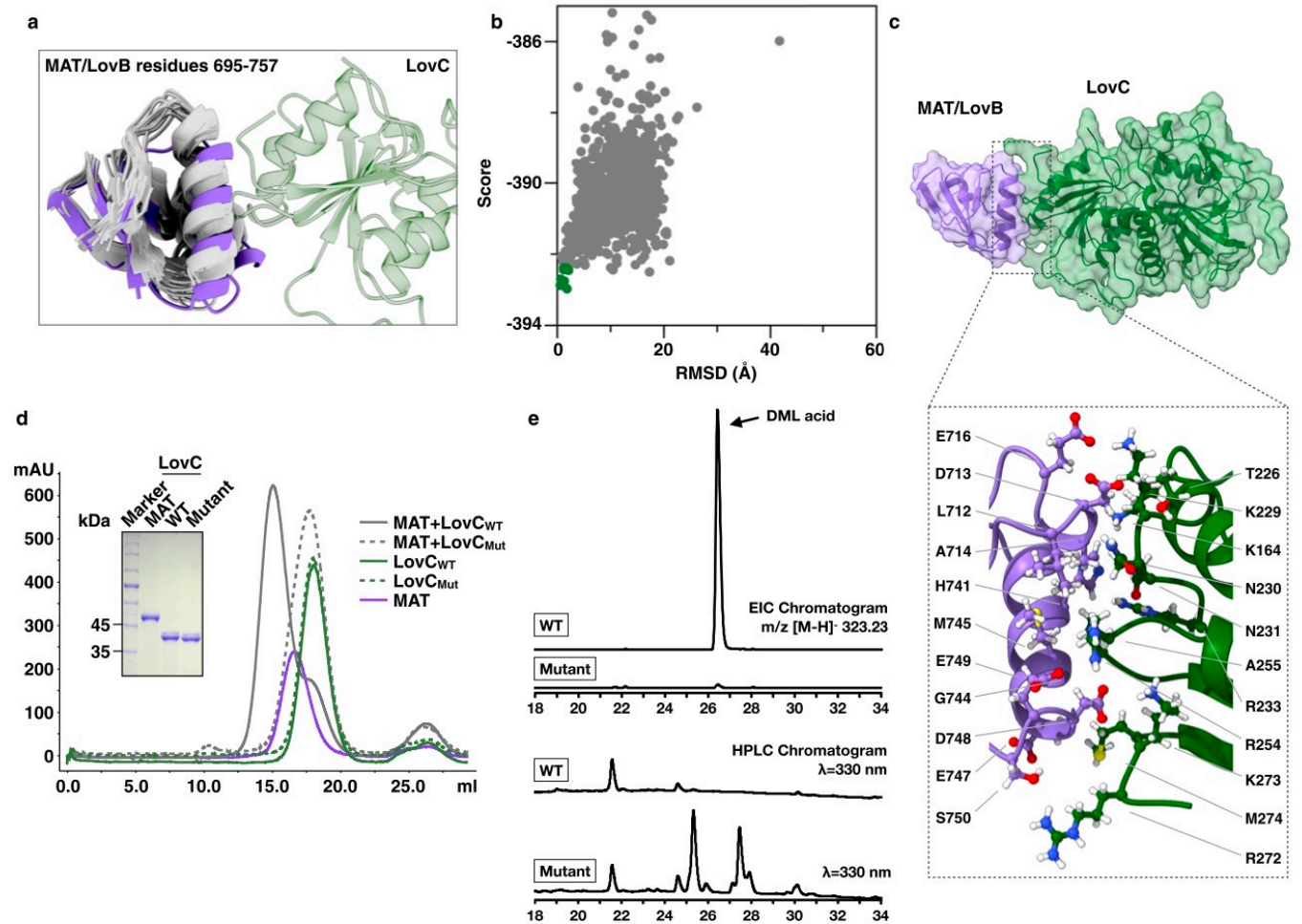
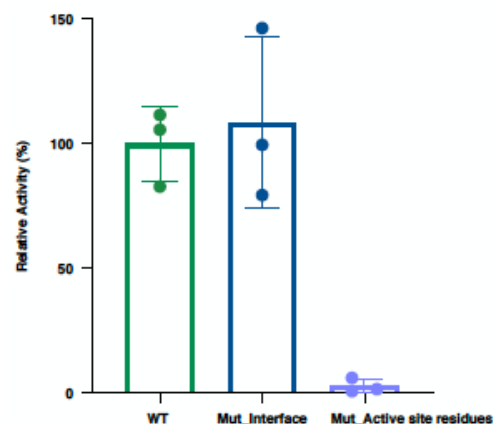


Fig. 4 Interaction between LovB and LovC is essential for the synthesis of DML. **a** Nineteen models built by RosettaCM were chosen for protein docking simulation with LovC. Residues 695–757 (part of the MAT domain) are shown. Purple color denotes the successful docked model. **b** Energy funnel for MAT/LovB-LovC docking analysis. The plot of score vs. rmsd shows the ten lowest-energy decoys (dark green) with rmsd <2.2 Å. **c** LovB-LovC interface. Top, view of the isolated electron density of MAT/LovB and interacting LovC with fitted molecular models. Bottom, close-up view of the interface between MAT/LovB and LovC (amino acids within 4 Å). **d** Size exclusion chromatography profiles for the interaction between LovC and the MAT domain of LovB. The LovC mutant profile is indicated by a dashed line. Elution of the component protein(s) is marked in color. One representative gel panel from at least three independent experiments shows the purified MAT domain of LovB, LovC, and the LovC mutant detected by SDS-PAGE. Source data is provided as a Source Data file. **e** HPLC traces showing the products of the in vitro reactions catalyzed by LovB with LovC or LovC mutant. LovG was included in the reaction mixture to release the final products. The DML acid has calculated and experimentally determined $m/z [M-H]^-$ values of 323.23 and 323.22, respectively. Top, the extracted-ion chromatogram profile; bottom, the HPLC chromatogram profile at $\lambda = 330$ nm.

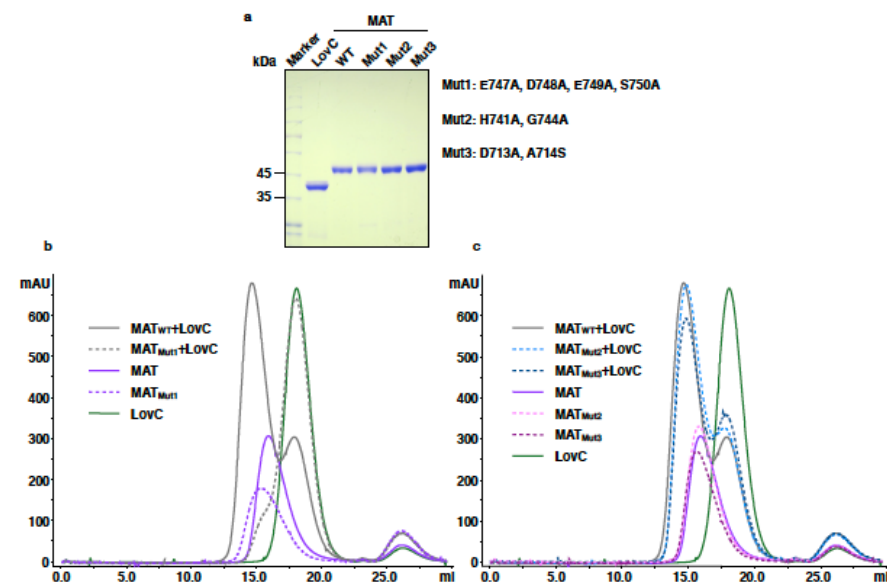
Interaction LovB_MAT-LovC

MAT-LovC interaction is essential for the synthesis of DML

- **Experimental** analyses: identification of the interaction interface
- Mutant MAT mut1 (E747A, D748A, E749A, S750A) is active but unable to interact with LovC (gel-filtration chromatography)



Supplementary Fig. 11 Activity assay of LovC interface mutant. The plot shows relative activities of LovC WT (—●—), the interface mutant (—●—) and the active site residues mutant (—●—). Error bars indicate standard deviations (\pm SD) from three biologically independent experiments ($n=3$). Source data are provided as a Source Data file.



Supplementary Fig. 10 Mutational analysis of the residues in the MAT domain mediating protein-protein interactions. The residues in the MAT domain mediating the interaction with LovC were mutated to alanine. **a** The purity of MAT domain protein mutants was analyzed using SDS-PAGE. One representative result from at least three independent experiments is shown. Source data is provided as a Source Data file. **b** Gel-filtration interaction study of MAT Mut1 with LovC. **c** Gel-filtration interaction study of MAT Mut2-3 with LovC.

Mechanism of transfer of the substrate between LovB domains and LovC mediated by the ACP domain

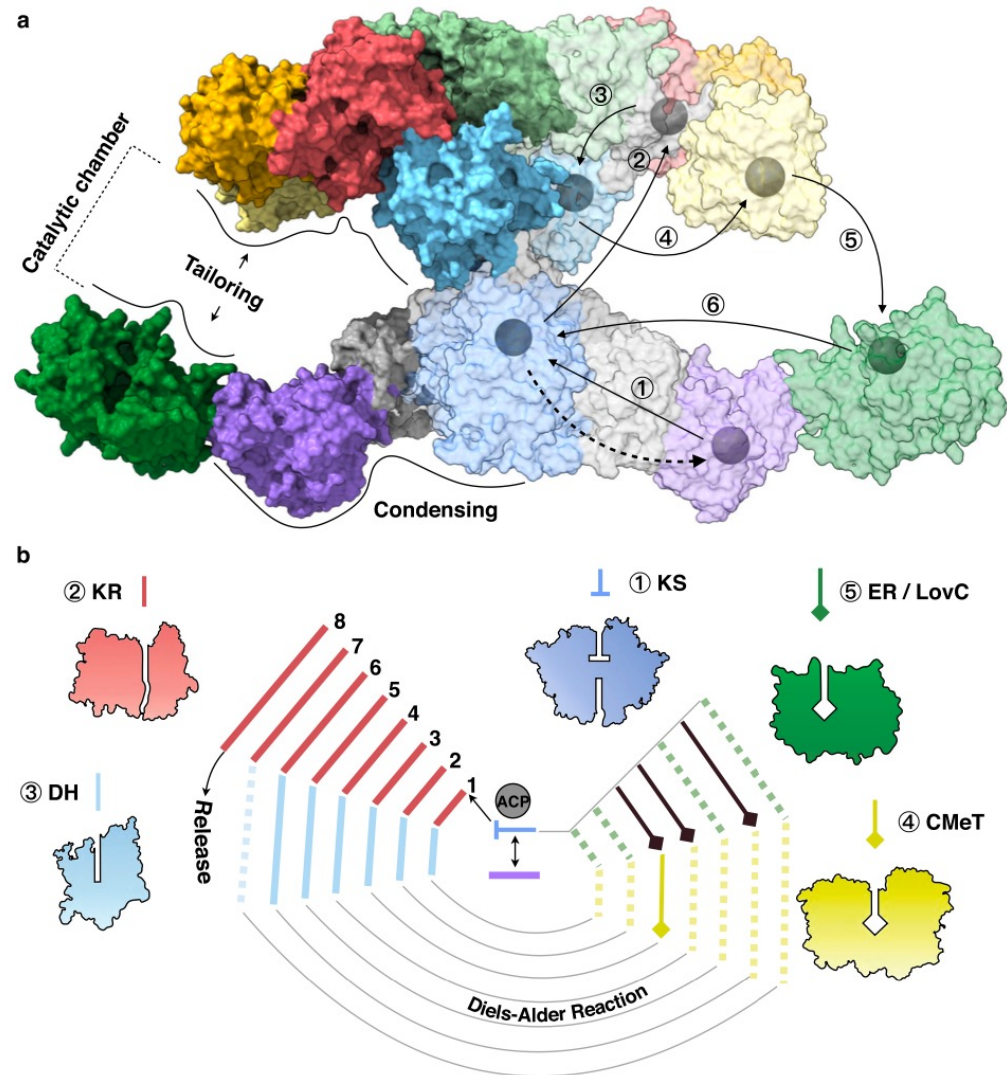
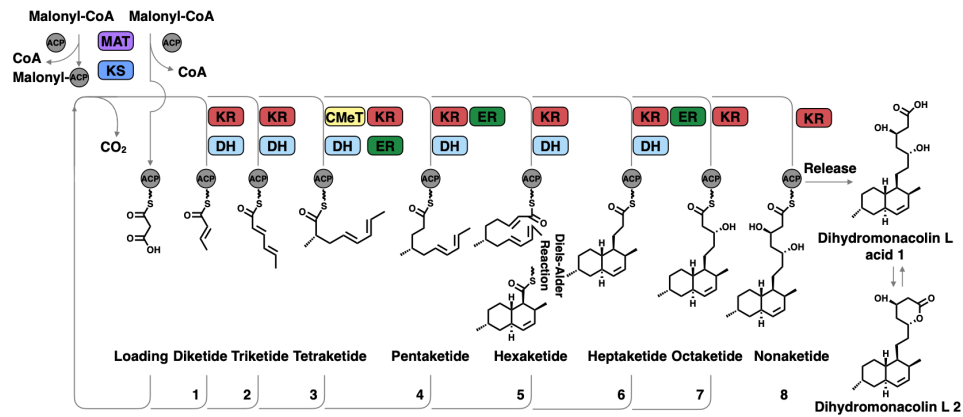


Fig. 5 Substrate shuttling within the catalytic chamber by the ACP domain. **a** The LovBC complex is shown as surface representation. The hypothetical substrate shuttling trajectories (one side) within the catalytic chamber are shown as lines with each arrow pointing towards the next step; the active site residues locations of each domain (depicted in Supplementary Fig. 13) are marked as gray balls. The dashed arrow indicates the loading of the malonyl precursor. **b** Schematic diagrams depicting the iterative, yet permutative function of LovB. After each condensation, the substrate undergoes different tailoring processes. The solid lines indicate the steps in which the intermediates are processed by the domain. The bypassed steps in each cycle are depicted in dashed lines.